



Developing an Empirical Model of Auroral Boundaries

Angeline G. Burrell¹

Gareth Chisham² , Bruce Fritz¹, Kate Zawdie¹

1: Naval Research Laboratory, Space Science Division, DC USA

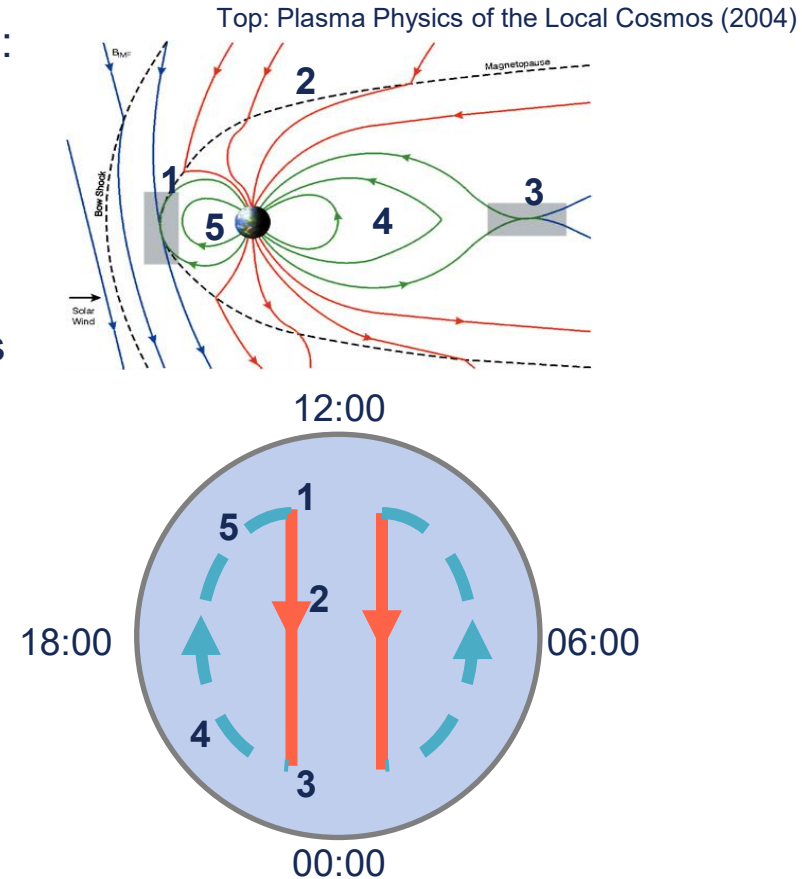
2: British Antarctic Survey, Cambridge UK

Outline

- Motivation
 - Background
 - Objective
- Boundary Data
 - Potential Observations
 - Individual Data Sets
- Boundary Model Construction
 - Data selection and weighting
 - Driver selection
 - Model formulation
- Products
 - Improved Gridding Data Sets
 - Boundary Identification Tool
- Conclusions
- Current and Future Work
- Acknowledgements

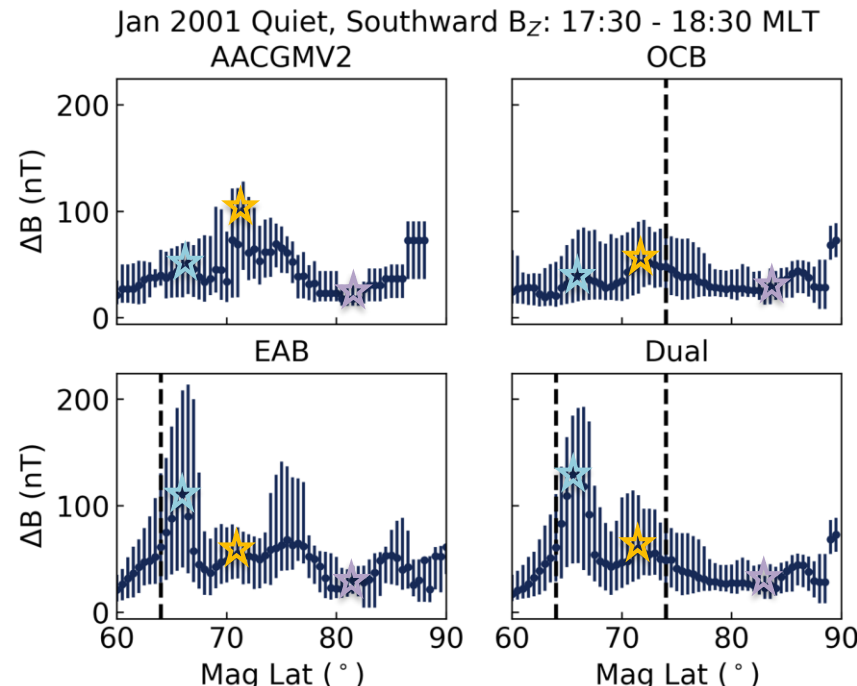
Motivation

- High latitude M-I coupling varies based on region:
 - Open field lines in the polar cap
 - Closed field lines in the auroral oval, high L-shells
 - Closed field lines below the auroral oval, low L-shells
- Magnetic coordinates can't accurately separate these regions, as they change based on changes in the Interplanetary Magnetic Field (IMF)
- Gridding relative to the polar cap (Open-Closed field line Boundary, OCB) and auroral oval (Equatorward Auroral Boundary, EAB) can improve modelling and statistical studies
- Providing EAB and OCB locations to ionospheric models can improve our high latitude specifications and magnetospheric coupling



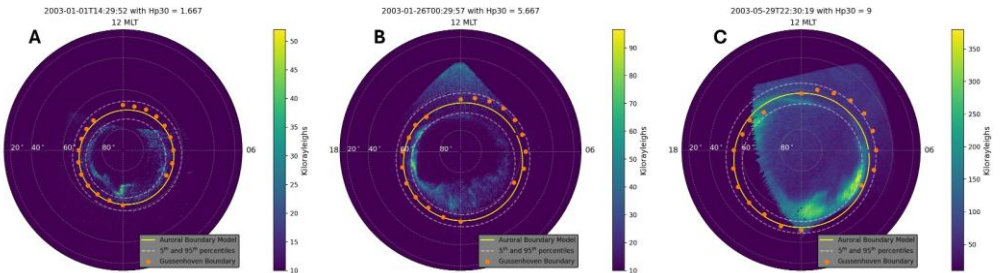
Adaptive Coordinate Systems

- The high latitudes at Earth consist of three physically distinct regions:
 - Polar cap
 - Auroral oval
 - Sub-auroral region
- Location of these regions change based on interactions between the solar wind and magnetosphere
- Treating the locations as static causes excessive smoothing and incorrect Atmosphere-Ionosphere-Magnetosphere (AIM) coupling
- Considering only one boundary is sufficient when in the polar cap or sub-auroral region



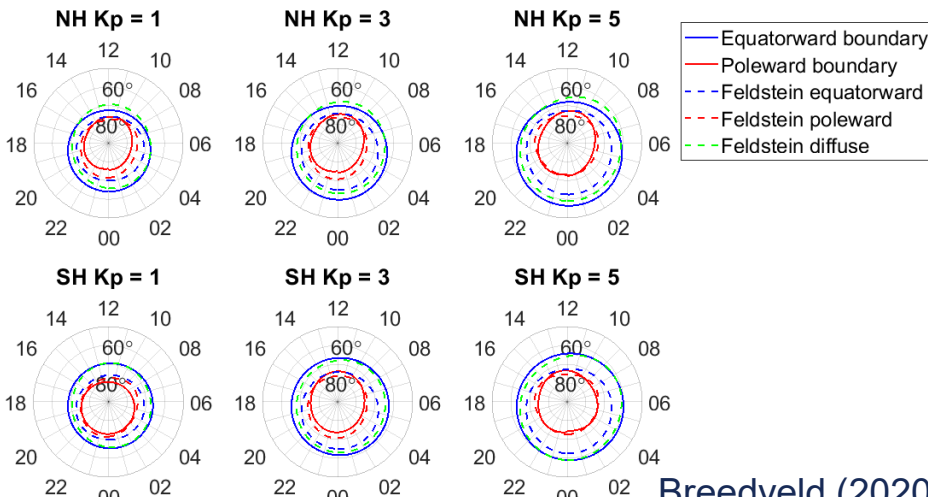
Goal: Model the OCB and EAB

- Requirements:
 - Available for public use
 - Specification of OCB and EAB in geodetic coordinates across all local times
 - Separate treatment for Northern and Southern hemispheres
 - Driven by appropriate solar and geomagnetic state specifications
 - Potentially provide an alternative version that can be driven by less-appropriate solar and geomagnetic state specifications that can be forecasted
- Current Options:
 - Models of auroral energy and probability
 - Models of particle precipitation
 - Private models of boundaries
 - Models of one boundary



Troyer et al. (2025)

TED Electrons < 20 keV Fourier Fit Model

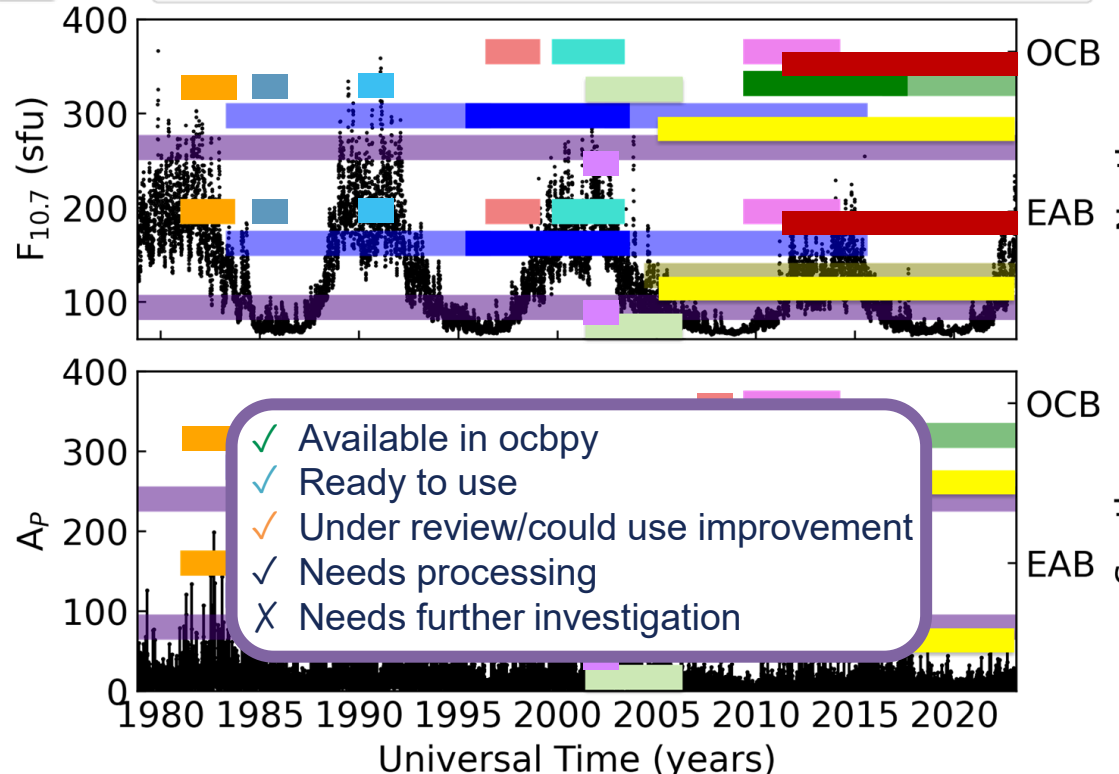
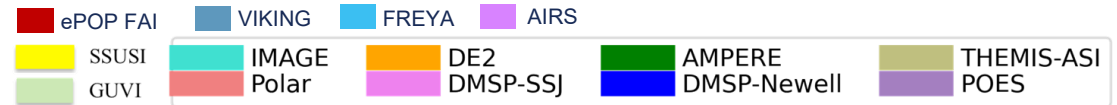


Breedveld (2020)

Potential Data for Boundary Model

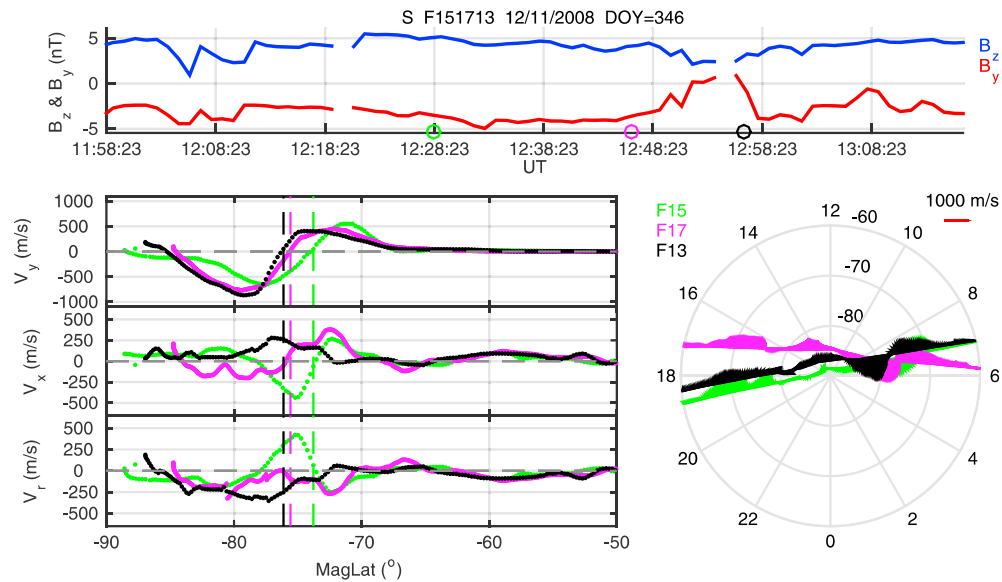
High latitude boundary measurements

- DMSP: OCB and EAB from SSJ (Newell boundaries, Kilcommons boundaries)
- DMSP: IVM measures Convection Reversal Boundary (CRB) along satellite track
- DMSP: SSUSI measures the auroral luminosity boundaries (ALBs)
- TIMED: GUVI measures the ALBs
- DE-2: particle precipitation boundaries (EAB and OCB)
- POES: have been used to get OCB/EAB
- AMPERE: R1/R2 current boundaries or R1peak (related to OCB), R2 peak, Heppner-Maynard Boundary (HMB) proxy
- IMAGE: ALBs in three wavelengths
- POLAR: ALBs
- Ground-based All Sky Imagers (ASIs): ALBs
- SuperDARN: CRB, HMB
- SuperMAG: can identify magnetic fluctuations associated with FACs
- AIRS: CO₂ imaging identified auroral boundaries
- VIKING (Swedish): ALBs
- FREYA: ALBs
- ePOP FAI: ALBs



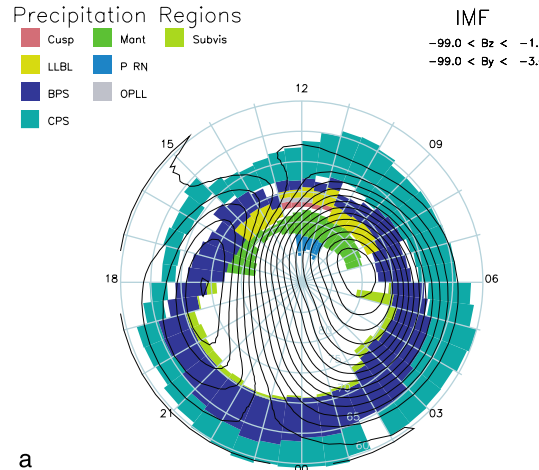
Boundary Data from DMSP IVM

- ✓ DMSP IVM (1998 – 2012)
 - Use the Ion Velocity Meter (IVM) to measure the cross-track drift and along-track in situ ion drift
 - Chen and Heelis (2017) describe the methodology used to produce this data set [source of figure]
 - Further work has produced an expanded data set that encompasses F11 – F18
 - *Useful for validating OCB near dawn and dusk MLT, where the two boundaries should move together*

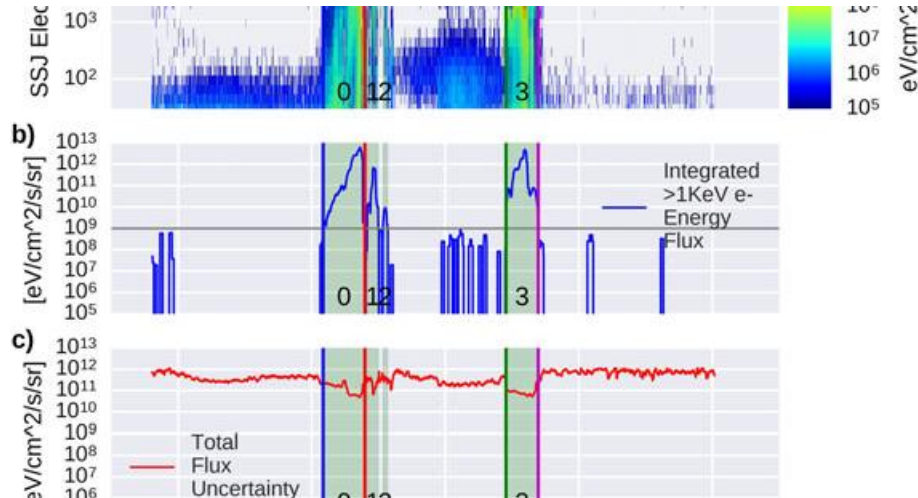


Boundary Data from DMSP SSJ

Newell Particle Precipitation Regions



Killcommons Particle Precipitation Boundaries



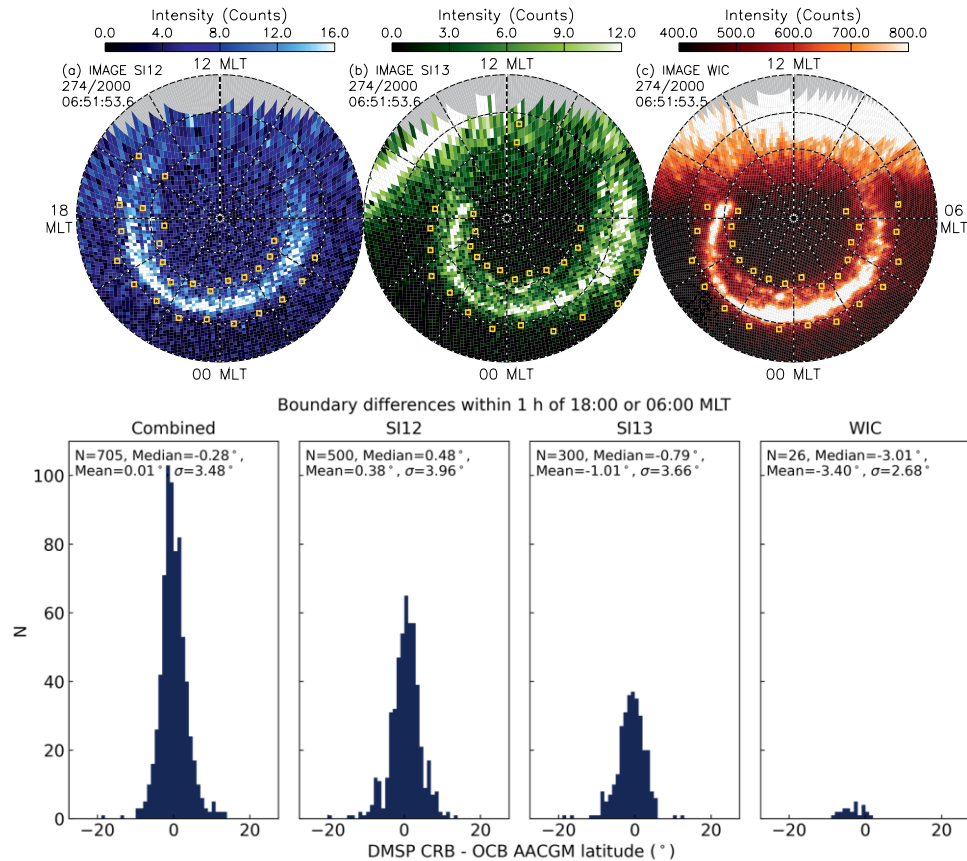
✓ DMSP SSJ (Newell: 1997 – 1998; Killcommons: 2010-2014)

- SSJ4 and SSJ5 measure the particle precipitation
- Newell et al. (2004) used SSJ to identify several different types of particle precipitation boundaries
- Killcommons et al. (2017) used SSJ with updated ephemeris to identify poleward and equatorward auroral boundaries based on particle precipitation
- *Useful for calibrating auroral luminosity boundaries and for model creation*

Boundary Data from IMAGE

✓ IMAGE (2000 – 2002)

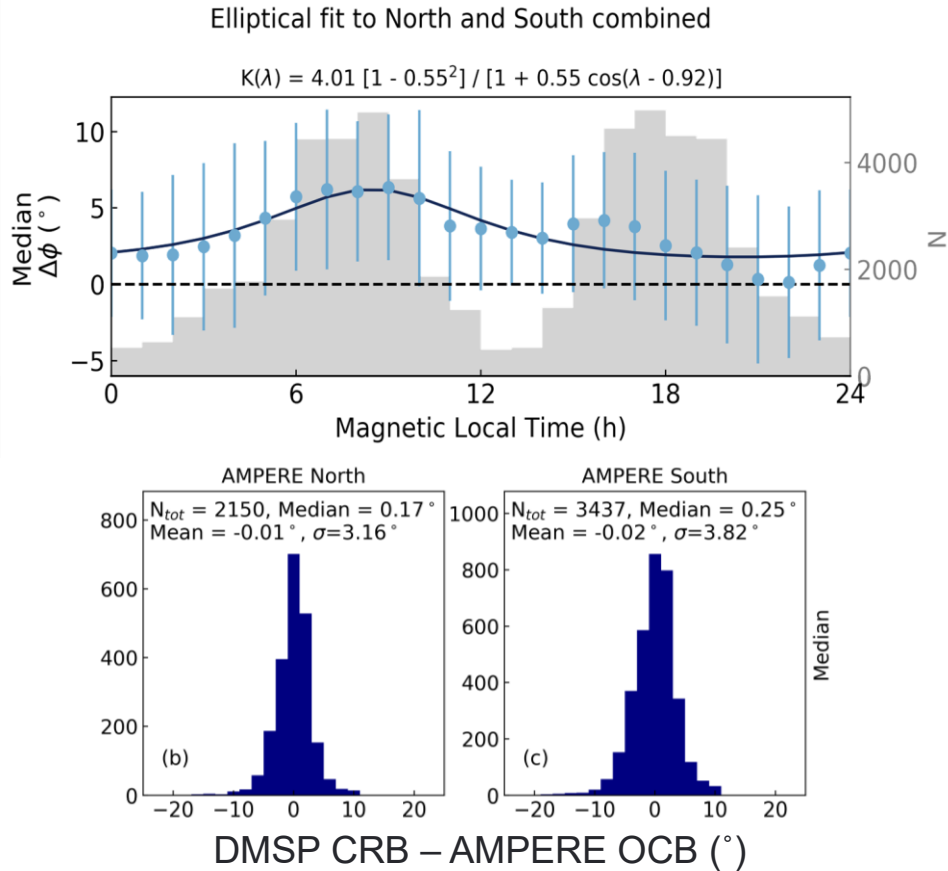
- SI12, SI13, and WIC measured Ly- α , O, and LBH emission bands in the Northern hemisphere
- Chisham et al., 2022 found the polar and equatorward ALBs and used Newell DMSP boundaries to determine the offset between the luminosity and precipitation boundaries
- Fits to the offset boundaries agree well with the DMSP CRB locations
- *Useful for model creation*



Boundary Data from AMPERE

✓ AMPERE (2010 – 2021)

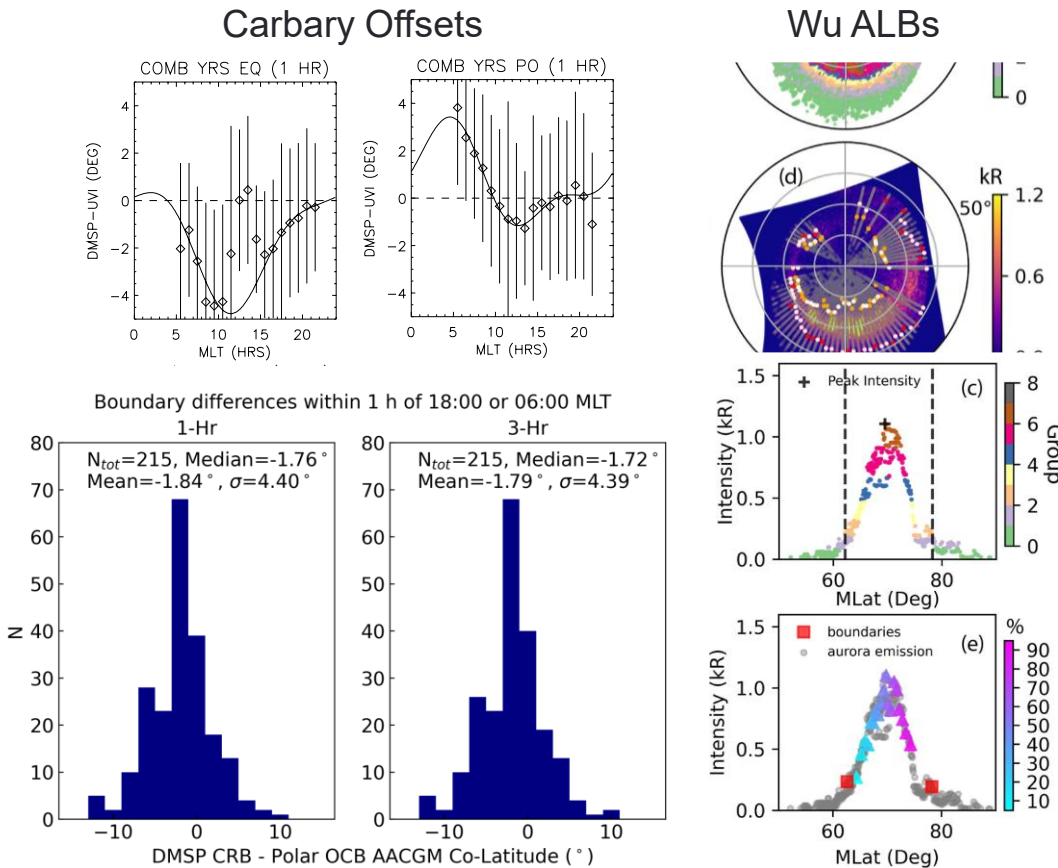
- AMPERE assimilates magnetic perturbation measurements to provide information about field-aligned currents (FACs) at the high latitudes
- Milan et al. (2015) used principle component analysis to identify different FAC boundaries
- Burrell et al. (2020) used the Killcommons SSJ boundaries to determine the offset between the OCB and R1/R2 current boundary
- Validated against DMSP CRBs
- *Useful for model creation*



Boundary Data from POLAR

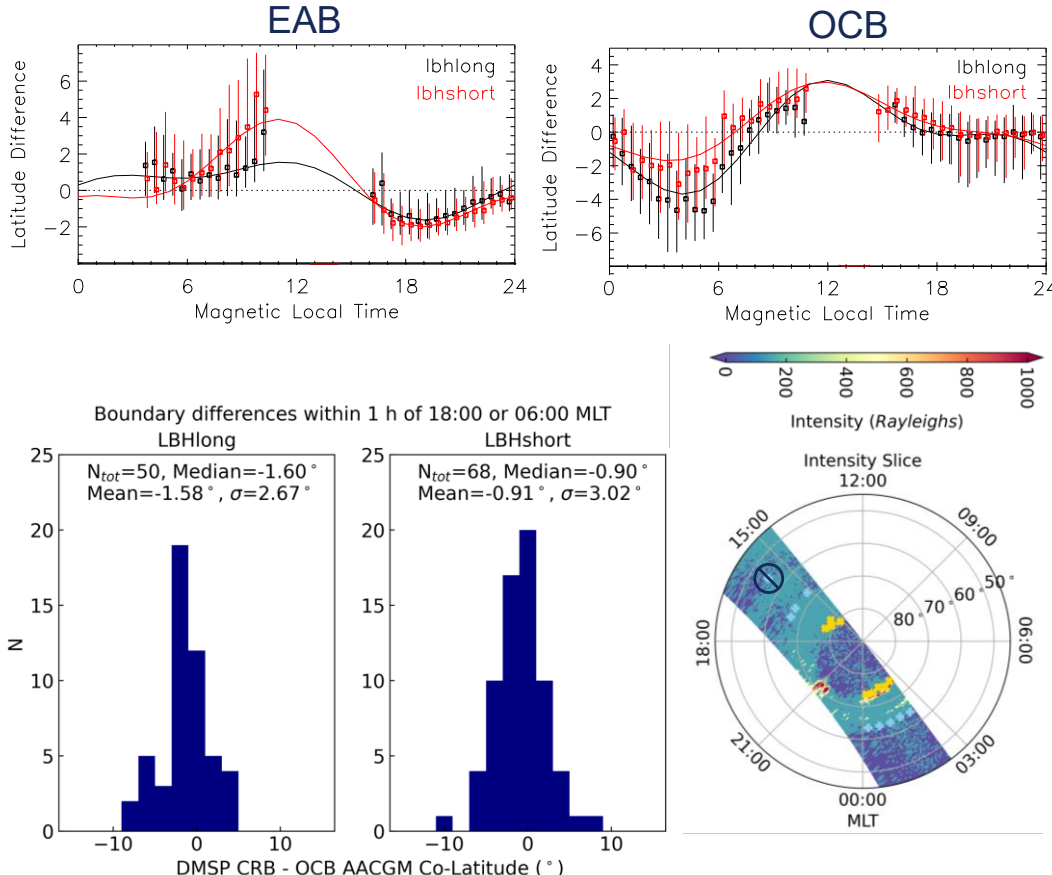
✓ POLAR (1997 – 1998)

- UVI measured LBHL and LBHS bands in the Northern hemisphere
- Carbary et al., (2003) used LBHL ALBs and Newell DMSP boundaries to determine the offset
- Wu et al. (2021) provided ALBs for both LBHL and LBHS
- Validation of fits to adjusted boundaries using DMSP CRBs shows a higher error than IMAGE
- *Useful for model creation*



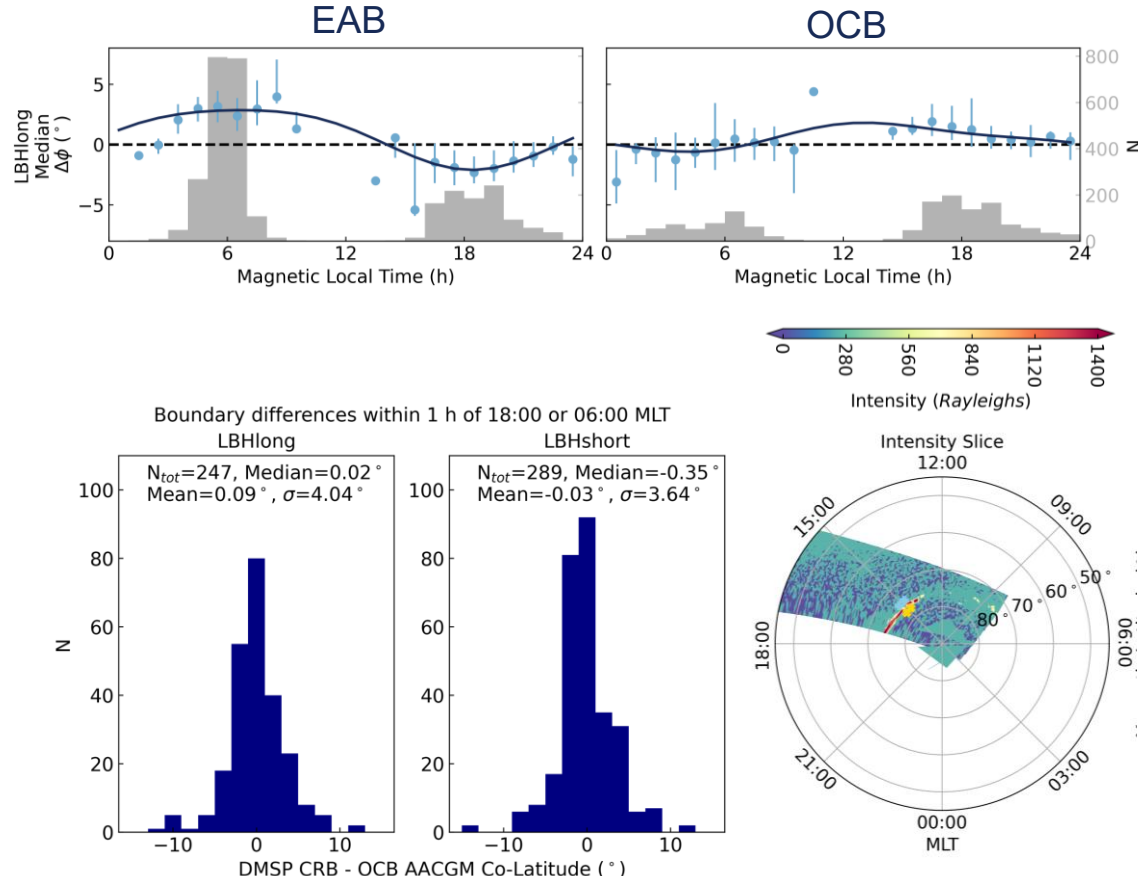
Boundary Data from GUVI

- ✓ **TIMED GUVI (2002 – 2007)**
 - Measured LBHL and LBHS bands in both hemispheres
 - NASA files provide auroral boundary identifications, but these boundaries do not match the intensity data well
 - Adapted the code described in Longden et al. (2009), into a new Python package `pyIntensityFeatures`
 - Paired with Newell boundaries to determine offset to particle boundaries
 - Validation performs better than POLAR, but worse than IMAGE
 - *Useful for model creation*



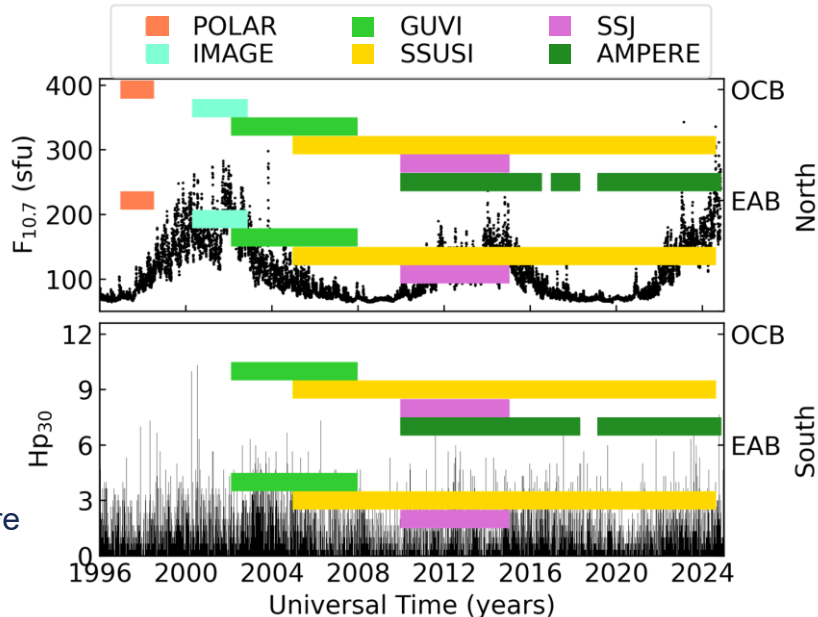
Boundary Data from SSUSI

- ✓ SSUSI (2005 – 2024)
 - Measured LBHL and LBHS bands in both hemispheres on F16, F17, F18, and F19
 - Similar format and issues as TIMED GUVI, used `pyIntensityFeatures` to identify ALBs
 - Paired ALBs with Kilcommons SSJ boundaries to determine EABs and OCBs in both hemispheres
 - Boundary validation shows similar accuracy as GUVI
 - *Useful for model creation*



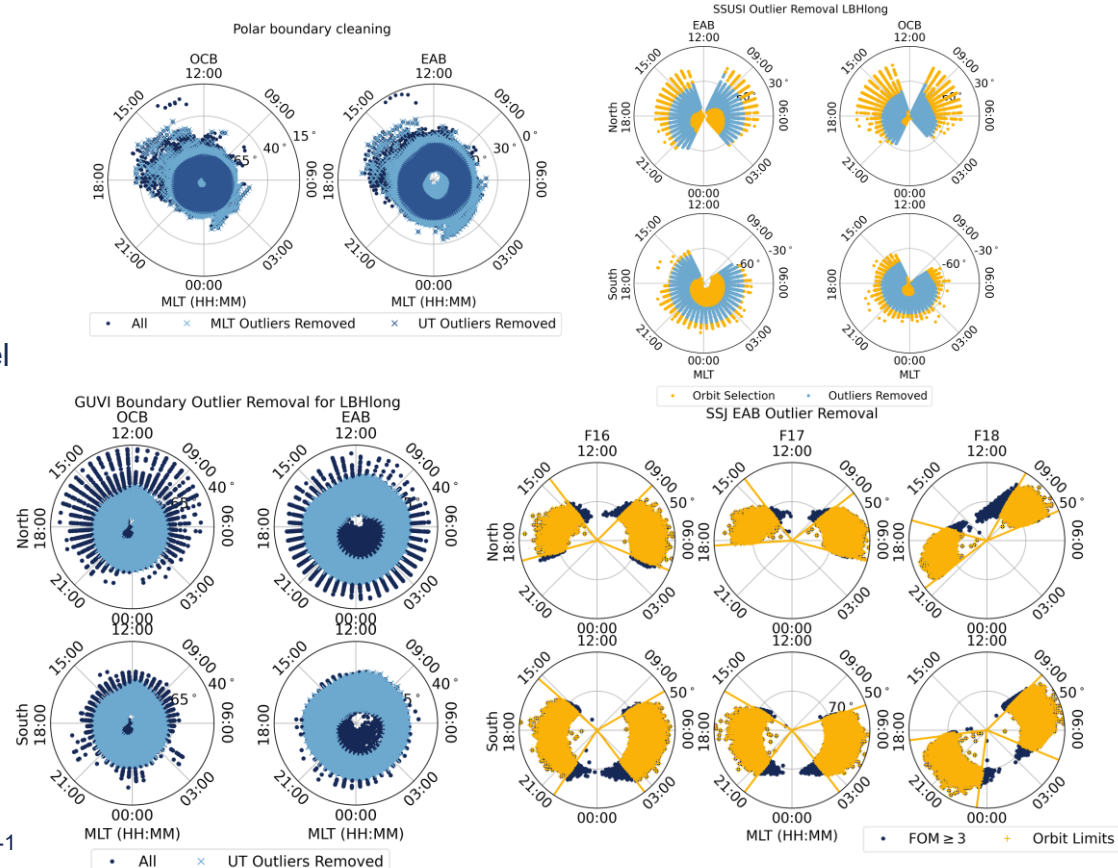
Gathered Boundaries and Drivers

- Boundary Data
 - Start with DMSP SSJ, AMPERE, IMAGE, POLAR, GUVI, and SSUSI
 - Covers about 2.5 solar cycles
 - Both EAB and OCB in both hemispheres
 - Calculate weight for each boundary using available quality metrics for the different data sets
 - Retain Newell boundaries for model validation
- Potential Model Drivers
 - Considering accuracy and forecastability
- Solar:
 - Day of year
 - Time of day
 - $F_{10.7}$
 - Cosmic ray counts
- Geomagnetic:
 - H_{p30}
 - AE
 - SMU
 - SML
 - SMR
 - IMF X, Y, and Z
 - IMF Clock Angle
 - Solar Wind Speed
 - Solar Wind Pressure
 - Solar Wind Density
 - Newell Coupling Function
 - Dipole moment



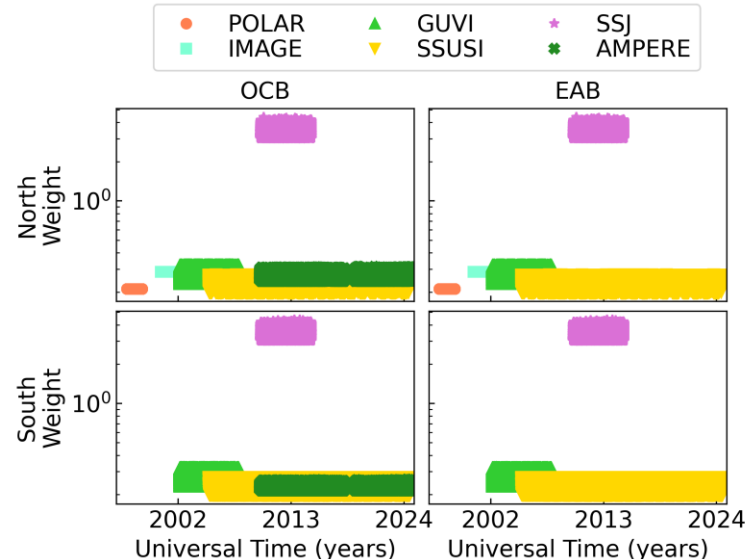
Outlier removal by Data Set

- POLAR
 - Remove outliers at each UT
 - Remove outliers at each MLT
- IMAGE
 - Outliers removed as described in Chisham et al. (2021)
- GUVI
 - Defined outlier quartiles and IQR using southern hemisphere data for each channel
 - Removed outliers at each MLT
- SSUSI
 - Removed boundaries in regions with a low occurrence, due to orbit
 - Removed outliers at each MLT and hemisphere
- SSJ
 - Removed boundaries with a FOM < 3
 - Removed boundaries in regions with low occurrence, due to orbit
- AMPERE
 - Removed boundaries with $\Delta J < 0.15 \text{ mA m}^{-1}$



Weights by Data Set

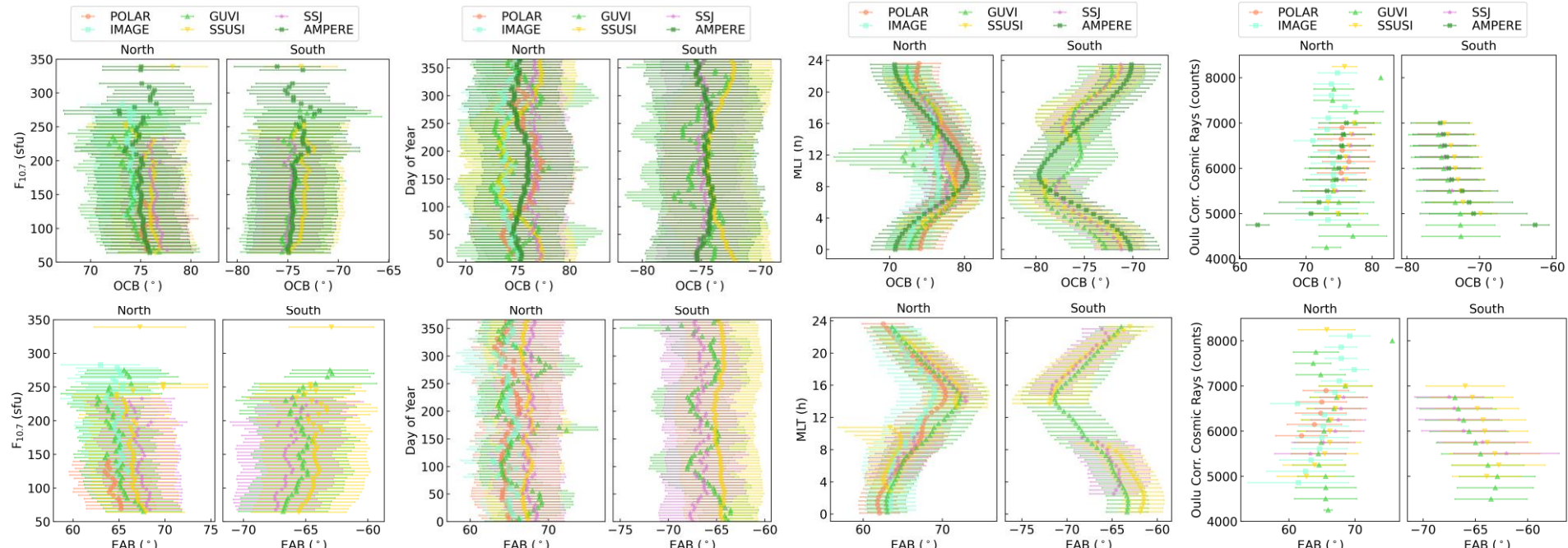
- Boundary weights should have higher values when data is more reliable
 - SSJ has a figure of merit for each boundary that is already appropriate as a weight
 - IMAGE and POLAR boundaries do not have individual uncertainties, so the weight was calculated using the median (q_2) and standard deviation (σ) from the CRB validation (1)
 - GUVI and SSUSI boundaries have individual uncertainties (ϵ), so their weight includes these along with the CRB validation (2)
 - AMPERE fits have current values that are used for quality control, with $\epsilon^2 = \Delta J^{-1}$, so these are combined with the CRB validation (2)



$$w = \frac{1}{\sqrt{q_{2_{CRB}}^2 + \sigma_{CRB}^2}} \quad (1)$$

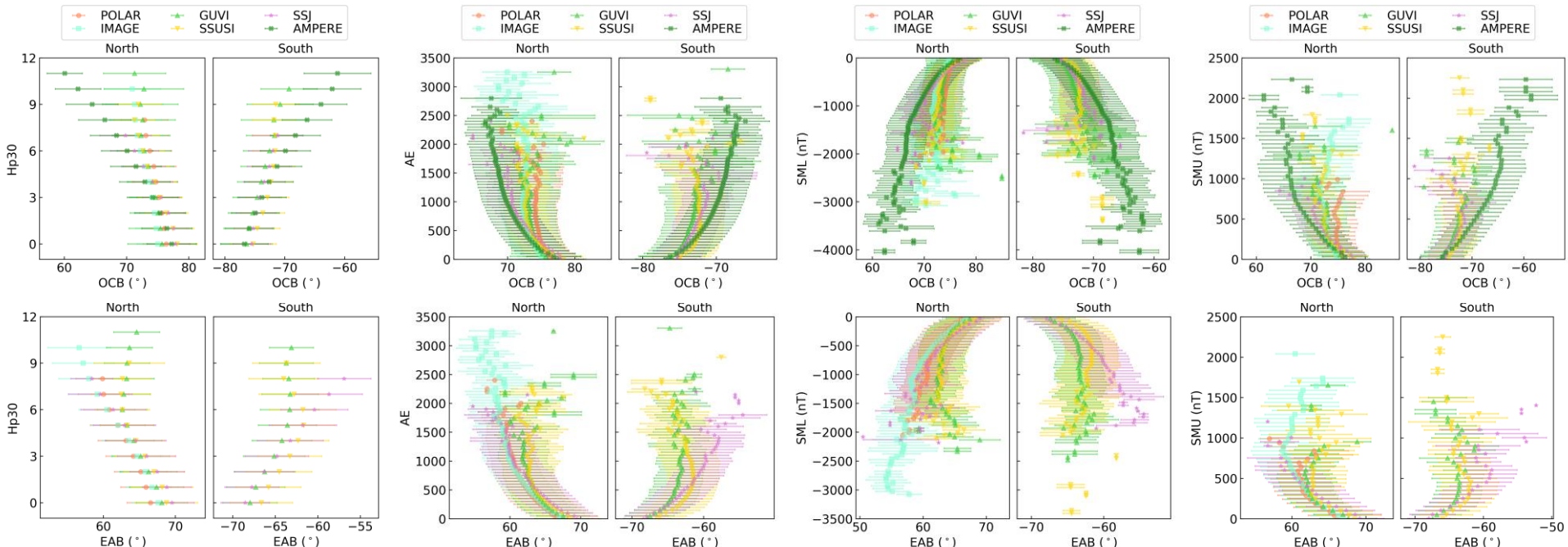
$$w = \frac{1}{\sqrt{q_{2_{CRB}}^2 + \sigma_{CRB}^2 + \epsilon^2}} \quad (2)$$

Driving Parameter Correlation: Solar



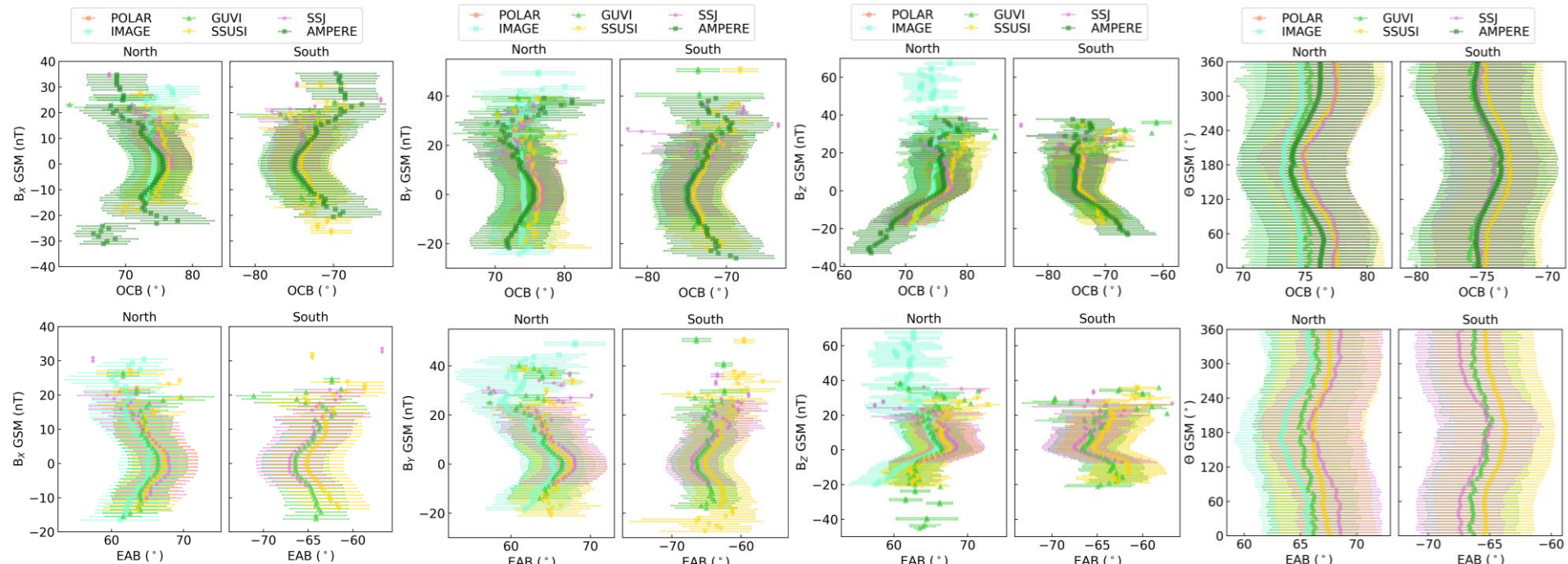
- Solar Variations are not key factors in determining the particle precipitation boundary locations
 - MLT has a strong diurnal variation

Driving Parameter Correlation: Geomagnetic



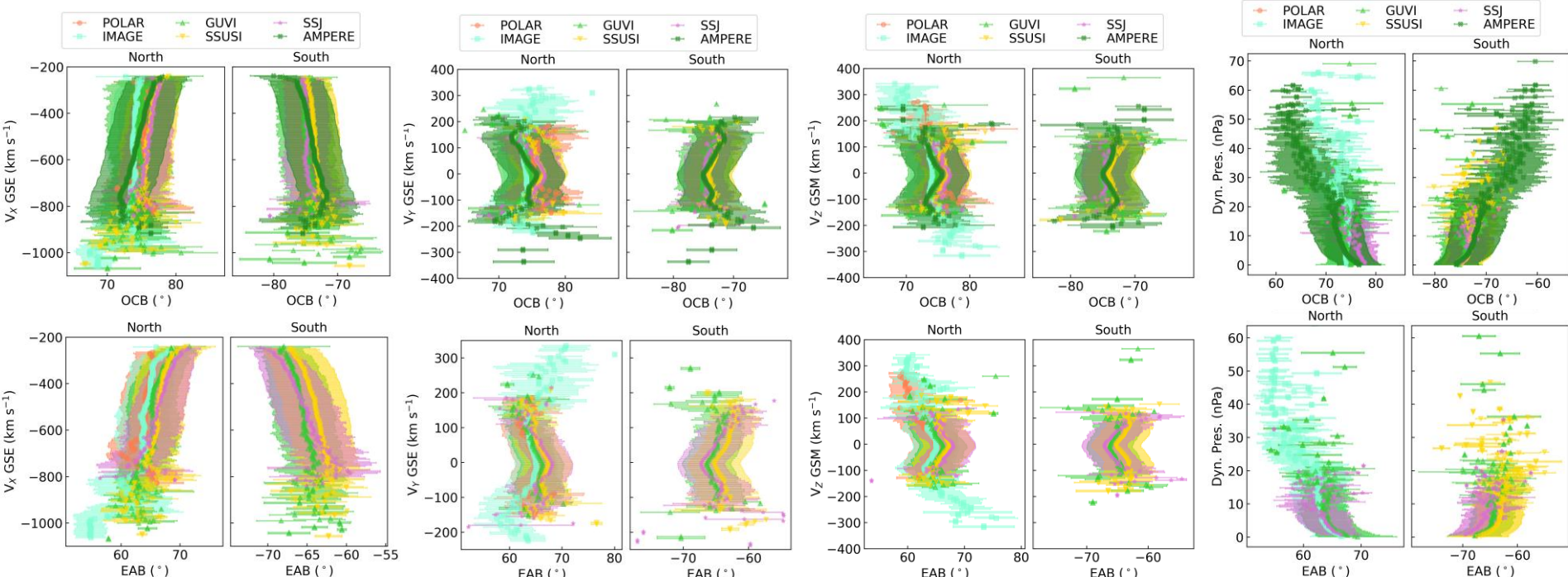
- Multiple geomagnetic parameters are correlated with particle precipitation boundary locations
- Northern and southern hemispheres respond similarly to the different magnetic drivers

Driving Parameter Correlation: IMF



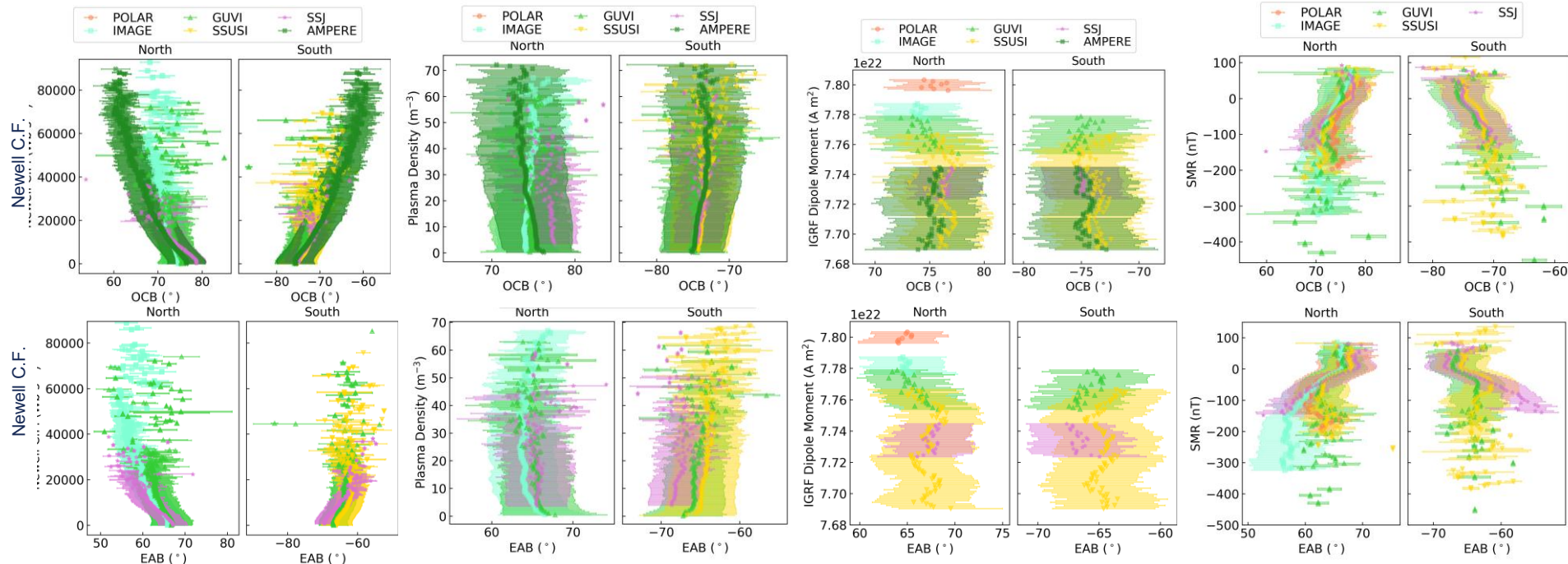
- IMF B_x and B_y response is well behaved about zero, while B_z shows a correlation with OCB for negative values
 - The clock angle (θ) shows a consistent correlation for OCB and EAB

Driving Parameter Correlation: Solar Wind



- V_x and dynamic pressure show the strongest correlation with OCB and EAB locations

Driving Parameter Correlation: More!



- The Newell Coupling Function ($d\Phi_{MP}/dt = C_{MP}v^{4/3}B_T^{2/3}\sin^{8/3}(\theta_c/2)$) shows the strongest correlation
- The main field's magnetic dipole moment, m_e , shows little variation with boundary location over this time period

Potential Model Formulations

Potential Methods

- Spherical harmonics

$$\phi_X = \prod_{i=0}^N \sum_{j=0}^M (a_{i,j} \cos j\omega_i + b_{i,j} \sin j\omega_i)$$

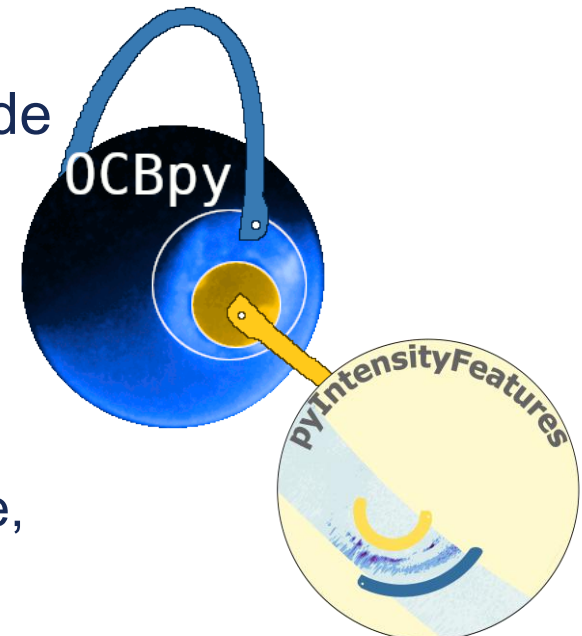
- ω_i initially includes:
 - MLT, Hp30, AE, θ , V_X , Dynamic Pressure, and Newell Coupling Function
 - ϕ_X is the boundary latitude, where X is OCB or EAB
- Machine learning tools
 - Need to investigate potential options

Potential Formulations

- Analyse impact of contributions from selected independent variables
 - Start with PCA
 - Manually add additional variables to determine impact
- Test formulations with hemispheres combined, separate, and as an independent variable
- Test formulation with magnetic and geodetic coordinates

Published Products

- Improved gridding data sets
 - Expanded OCBpy to grid in dual-boundary coordinates
 - Updated AMPERE boundaries in OCBpy
- Formalized Longden boundary detection code
 - Generalized methodology
 - Allow any number of multi-Gaussian fits
 - Added adaptive limits for partial-aurora scans
 - Added test for MLT consistency in boundary IDs
 - Developed a unit test suite
 - Available as a pip-installable Python package, `pyIntensityFeatures`



Conclusions

- Implementing adaptive, high latitude coordinates would improve research efforts for terrestrial atmospheric, ionospheric, and magnetospheric physics
 - Standard magnetic coordinates combine data from the polar cap and auroral regions, even for a narrow selection of solar and geomagnetic conditions
 - Considering only one boundary is sufficient when examining the region well-defined by that boundary
 - Dual-boundary gridding does the best job of fully specifying the high-latitude features
 - An open-source model of the polar cap and equatorward auroral oval will improve high latitude statistical studies, empirical model construction, and energy boundaries in first-principles models

Current and Future Work

- Publish Results
 - New boundaries and boundary validations
 - POLAR, GUVI, SSUSI
 - Make appropriate data sets available on OCBpy
 - `pyIntensityFeatures` manuscript under review
- Creating an empirical boundary model
 - Combining DMSP SSJ, AMPERE, IMAGE, POLAR, GUVI, and SSUSI
 - Covers about 2.5 solar cycles
 - Both EAB and OCB in both hemispheres
 - Retaining DMSP Newell boundaries for validation
 - Selected a subset of geomagnetic parameters to consider in model formulation
 - Considering different empirical model construction methods

Acknowledgements

SuperMAG data was obtained from <http://supermag.jhuapl.edu/>. For the ground magnetometer data we gratefully acknowledge: For the ground magnetometer data we gratefully acknowledge: INTERMAGNET, Alan Thomson; CARISMA, PI Ian Mann; CANMOS, Geomagnetism Unit of the Geological Survey of Canada; The S-RAMP Database, PI K. Yumoto and Dr. K. Shiokawa; The SPIDR database; AARI, PI Oleg Troschichev; The MACCS program, PI M. Engebretson; GIMA; MEASURE, UCLA IGPP and Florida Institute of Technology; SAMBA, PI Efthyia Zesta; 210 Chain, PI K. Yumoto; SAMNET, PI Farideh Honary; IMAGE, PI Liisa Juusola; Finnish Meteorological Institute, PI Liisa Juusola; Sodankylä Geophysical Observatory, PI Tero Raita; UiT the Arctic University of Norway, Tromsø Geophysical Observatory, PI Magnar G. Johnsen; GFZ German Research Centre For Geosciences, PI Jürgen Matzka; Institute of Geophysics, Polish Academy of Sciences, PI Anne Neska and Jan Reda; Polar Geophysical Institute, PI Alexander Yahnin and Yarolav Sakharov; Geological Survey of Sweden, PI Gerhard Schwarz; Swedish Institute of Space Physics, PI Masatoshi Yamauchi; AUTUMN, PI Martin Connors; DTU Space, Thom Edwards and PI Anna Willer; South Pole and McMurdo Magnetometer, PI's Louis J. Lanzarotti and Alan T. Weatherwax; ICESTAR; RAPIDMAG; British Artarctic Survey; McMac, PI Dr. Peter Chi; BGS, PI Dr. Susan Macmillan; Pushkov Institute of Terrestrial Magnetism, Ionosphere and Radio Wave Propagation (IZMIRAN); MFGI, PI B. Heilig; University of L'Aquila, PI M. Vellante; BCMT, V. Lesur and A. Chambodut; Data obtained in cooperation with Geoscience Australia, PI Andrew Lewis; PENGUIn, co-PIs Bob Clauer, Michael Hartinger, and Zhonghua Xu; MagStar, PI Jennifer Gannon; LISN PI Cesar Valladares; SuperMAG, PI Jesper W. Gjerloev; Data obtained in cooperation with the Australian Bureau of Meteorology, PI Richard Marshall.

OMNI Solar Wind data are courtesy of OMNI and are the 1-min-averaged, field/plasma data sets shifted to the Earth's bow shock nose (BSN). This "High Resolution OMNI" (HRO) data set involves an interspersal of BSN-shifted ACE, Wind, IMP 8 and Geotail data. See https://omniweb.sci.gsfc.nasa.gov/ow_min.html, Dr. Natalia Papitashvili, Mail Code 672, NASA/Goddard Space Flight Center, Greenbelt, MD 20771.

Cosmic Ray data were obtained from <https://cosmicrays.oulu.fi/>, which is supported by the Sodankyla Geophysical Observatory.

Hp30 data was provided by the GFZ Helmholtz Centre for Geosciences.

F10.7 data was provided from two sources: the NOAA radio flux obtained through LISIRD and the radio flux prepared by the U.S. Dept. of Commerce, NOAA, Space Weather Prediction Center

TIMED GUVI and **DMSP SSUSI** data were provided through CDAWeb.

AGB, KAZ, and BF were supported by the **Office of Naval Research**

angeline.g.burrell.civ@us.navy.mil

Adaptive Coordinate Approaches

- Single Instrument or Platform
 - Grid data from the same instrument or other instruments on the same platform relative to an appropriate boundary observed at that time
- Multi Instrument
 - Grid data observed at the same time and region as another observation of an appropriate boundary
- OCBpy
 - Tool to grid data in adaptive coordinates (OCB, EAB, or Dual Boundary)
 - Provides access to multiple boundary data sets
 - A model of OCB and EAB locations would allow greater usage of adaptive coordinates

DMSP Southern O⁺ Downflow: Redmon et al. (2010)

